SPECIAL PROJECT FINAL REPORT

All the following mandatory information needs to be provided.

Project Title:	Use and value of ECMWF short-range and seasonal forecast products for developing countries in terms of end-user impact variables
Computer Project Account:	spitP4DC
Start Year - End Year :	2013 - 2015
Principal Investigator(s)	Adrian Mark Tompkins
Affiliation/Address:	Abdus Salam International Centre for Theoretical Physics (ICTP), Strada Costiera 11, Trieste ITALY
Other Researchers (Name/Affiliation):	Francesca Di Giuseppe (ECMWF) Gulilat Tefera Diro (current affiliation UQAM) Felipe Colon Gonzalez (current affiliation UEA)

Special Project SPITP4DC final report for period 2013-2015

Adrian Mark Tompkins[1,*],

1 Earth System Physics, The Abdus Salam International Centre for Theoretical Physics (ICTP), Strada Costiera 11, Trieste, Italy

* tompkins@ictp.it

Summary of Project Objectives

This special project aimed to develop a coupled disease modelling system for malaria in Africa and test the capability of the system to predict malaria transmission anomalies up to four months ahead. The specific aims were to complete the coupling of the VECTRI malaria model to the monthly EPS system and the seasonal system SYS4 in a seamless system. This prediction system would then be validated for the focus areas of Eastern Africa, Malawi, and possibly West Africa (Ghana and Senegal) where health data resources allowed. The potential predictability gain available by introducing further developments of the VECTRI was to be quantified. The aim by the project end was to have a working prototype seasonal prediction system for malaria

Summary of Problems Encountered

Permission restrictions to near real-time forecasting data proved to be problematic. While all the validation was performed using the hindcast period, the aim was to set up the system in such a way that it could be converted to a pilot operational suite with ease. As this meant setting up the SMS suite to use operational forecasts, the consequence

Experience with the Special Project Framework

Concerning the SPF, I can only repeat my summary of the last report, namely that the facilities at ECMWF are second to none, and where teething problems occur setting up scripts and code on the ECMWF system, the staff at ECMWF were always extremely helpful.

Summary of the results

Modelling system

The basic modelling system was described in Tompkins and Di Giuseppe (2015b) and the following system overview is adapted from that publication.

The Malaria early warning system (MEWS) consists of two modelling components: a weather forecasting system and a dynamical malaria model (Fig. 1). The first 32 days of the weather forecast uses temperature and precipitation provided by the EPS (Vitart et al., 2008). From day 33, the forecasts of the lower resolution and longer-range system 4 seasonal forecasting system (Molteni et al., 2011) are used for the remainder of the

four month forecast. Individual forecasts starting from slightly different initial conditions in order to sample forecast uncertainty.

Temperature from both systems is adjusted using correction of the mean bias as a function of location, calendar month and forecast lead-time with respect to the analysis data and subsequently statistically downscaled to the 27km resolution using a fixed lapse rate correction to account for the topography (Giorgi et al., 2003). This resolution is adequately fine to allow aggregation for comparison to district level health data if required. The precipitation is also downscaled to this resolution using first order conservative remapping (described in Jones, 1999). One weakness of this first generation system is that the precipitation forecasts are not presently bias corrected, implying that the mean simulated malaria transmission will be subject systematic biases that can be caused by misplaced monsoon locations (e.g. see analysis of the earlier SYS3 in Tompkins and Feudale, 2010) or mis-timed rain onsets (Diro et al., 2012, examined SYS3 performance in the horn of Africa). The resulting daily precipitation and temperature forecasts are then used to drive the VECTRI dynamical malaria model (Tompkins and Ermert, 2013), to produce an ensemble of forecasts of a range of epidemiological and entomological measures.

The malaria model is initialized from realistic initial conditions. The malaria forecasting system requires an assessment of the important entomological and epidemiological variables such as vector adult and larvae density, the circumsporozoite protein rate (CSPR), and parasite ratio, in addition to the surface hydrological state giving the availability of breeding sites, to initialize the malaria modelling component correctly. Without this step the malaria model would suffer from so-called 'spin up' in the first weeks of the forecast, as the model adjusts from idealized initial conditions, and valuable information concerning the climate conditions prior to the forecast start would be lost. The malaria analysis does not incorporate health or entomological observations. This is due to the fact that direct observations of entomological variables are not generally available as they are collected in isolated research projects, and are in any case not available in near-real time required for an operational framework.

We designed the analysis system using temperature and precipitation from the operational ERA-Interim reanalysis system of ECMWF (Dee et al., 2011) to drive the malaria model and provide malaria analyses of the relevant variables for each day from 1981 to the present. Precipitation is taken from a short range 24 hour forecast starting from each 00Z analysis cycle. The resulting analyses are used to provide initial conditions for each malaria forecast. Thus if a forecast starts mid-way in a wetter than usual season, for example, the initial conditions will reflect this in terms of greater vector and larvae densities and more breeding sites available. The skill of the malaria forecasts is consequently not only impacted by the skill of the climate forecasts, but also in part derives from the knowledge of the climate anomalies that occurred prior to the forecast start that is contained in the malaria analysis system. To our best knowledge, this is the first such dynamical forecasting system that attempts to fully initialize the malaria model component from an analysis system.

The choice of using reanalysis for this task was made with operational requirements in mind. Firstly, it combines the available sparse, in situ measurements with the continuously changing remotely sensed information into a self-consistent assessment of the atmospheric state, thus maximizing continuity over time while ensuring continual spatial coverage and near real-time operational delivery. For temperature, in situ measurements are sparse in many regions in Africa, or not available on the global telecommunications system (GTS) in real-time. In any case, despite documented biases in the distribution of rainfall intensity and the rainfall mean, the reanalysis derived rainfall is nevertheless capable of representing the intraseasonal variability over Africa, with Thiemig et al. (2012) demonstrating its competitiveness with some satellite-based
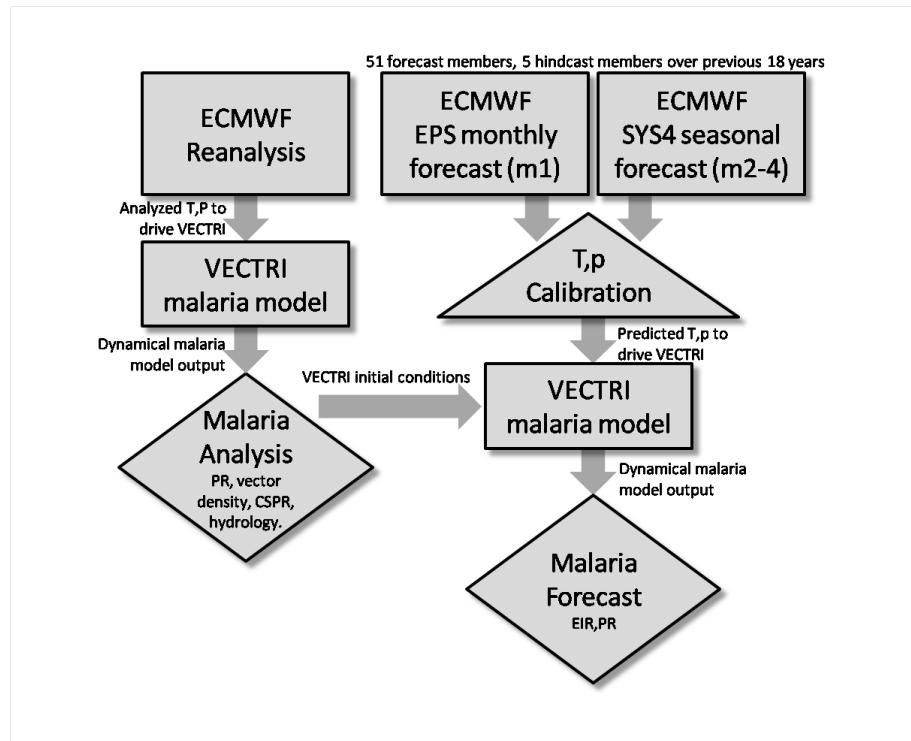
Figure 1. Schematic of the forecast system set up, with boxes representing models, triangles for processes, and diamonds used for products. The operational numerical weather prediction reanalysis of temperature and rainfall is used to drive the malaria model to provide a malaria analysis of epidemiological and entomological indicators (PR=parasite ratio, CSPR=Circumsporozoite Protein Rate), which are used as initial conditions for the forecast. The malaria forecast uses climate information from the high resolution monthly ensemble prediction system (EPS) climate forecasts in the first month (m1, consisting of days 1-32), which is seamlessly combined with the seasonal forecast system for m2-4. Both precipitation (P) and temperature(T) are rescaled, and temperature calibrated before application to the malaria model, which then provides forecasts of PR and entomological inoculation rate (EIR).

products. Dutra et al. (2013) found that ERA Interim rainfall could be successfully used in drought monitoring.

Evaluation

To illustrate the potential value of the system in a real epidemic scenario, we examined the past performance over the east African highlands. The outpatient data of highland regions of south-west Uganda and western Kenya have received considerable attention in the literature. In fact, in their comprehensive review of articles examining the relationship between climate and malaria, Mabaso and Ndlovu (2012) found that this region was the most studied. Table 1 gives a qualitative and brief summary of the key malaria transmission anomalies in highlands of either Western Kenya and/or Uganda between 1995 and 2010. The summary of the data is that a significant epidemic occurred in early 1998 across the region in the highlands that has been extensively described and linked the the major El Niño event of 1997/1998 (Lindblade et al., 1999; Githeko and Ndegwa, 2001; Alonso et al., 2011). The other articles cited described evidence of more minor anomalies in transmission during 1994-5, 2002, 2005, 2006 and

2009/2010, with the term 'minor' employed in a broad sense to variously imply short-lived, less intense or geographically restricted outbreaks.

To make an initial qualitative comparison to the forecasting system, the average normalized value of the ensemble mean predicted ln(EIR) is analyzed for all points at heights exceeding 1500m (the results were insensitive to this altitude threshold) in a region spanning 28-36E and 2S to 2N, with each month considered separately to remove the annual cycle of malaria transmission. A running mean is also applied of 5 months[1]. The forecast timeseries is then classified into three alert levels, where an amber alert signifies an upper tercile event, while a red alert level signifies a value exceeding the 90th percentile. We emphasize that these tercile thresholds are chosen as they are commonly employed in meteorological forecasting circumstances, but may have little relevance to the decision-making process of, for example, a national malaria control program. A full cost-loss analysis of suitable interventions is required to determine suitable thresholds for action, and thus the alert levels should be strictly viewed as indicative and illustrative.

The resulting timeseries (Fig. 2) is encouraging as it clearly shows that the major outbreak starting February 1998 is predicted four months ahead and is by far the most significant event predict predicted during the period 1995 to 2012, in qualitative agreement with the observations. In addition, all forecast lead times indicate lesser events occurring in 1995, 2002, 2005, 2006 and 2009/2010. However, on closer examination, it is clear that the timing of the predicted events is often inaccurate. While the main 1998 event is predicted to reach the highest alert level in February/March 1998, the event appears to last too long, with the alert level remaining throughout 1998. Likewise, the event is 2005 appears well predicted 4 months in advance, but is weaker and too early in the shorter lead time forecasts. High levels of transmission in 2006 appear to continue into 2007, which does not appear to be confirmed in the literature. Moreover, in general there is a tendency for epidemic alerts to occur earlier in time in the shorter range forecasts (for example, 2002, 2005, 2006/2007 and 2010). This could be related to a drift in the bias characteristics of the forecast precipitation which is presently not bias corrected in the system. In summary, while the system shows promise at predicting during which years epidemic conditions are likely to occur, there remains much to be done to improve the representation of sub-seasonal fluctuations in transmission, while again emphasizing the highly qualitative nature of this initial comparison which amalgamates all highland areas in Uganda and Western Kenya into a simple single index.

Predictability of malaria

The skill of the forecast is examined for both the climate and malaria forecasts using the operational forecast system output for 2012. We analyze the forecasts of 2012, and the 18 years of hindcasts, giving an evaluation period of 1994 to 2012. Although ideally one would evaluate an ensemble system using probabilistic skill scores, the small ensemble size of the hindcast (5 members) prevents this and thus the analysis is made for the skill of the ensemble mean anomaly correlation (Murphy and Epstein, 1989). Temperature and calibrated precipitation are validated against the ERA-Interim reanalyses. We identify the locations where skill in predicting malaria transmission is statistically significant one to four months in advance (referred to hereafter as 'potential malaria prediction skill') for each calendar month (Fig. 3). In addition to malaria, we show the skill in predicting anomalies of rainfall and temperature to identify which of these variables generate any identified malaria prediction skill.

---

[1]This simple smoothing using a centered filter window could not be applied in real-time forecasting scenario as the future months are not available.

Table 1. Summary of selected literature that discuss epidemic conditions in the highlands of Uganda, west Kenya or Tanzania

Year	Reference	Summary
1994	Alonso et al. (2011)	Higher than usual transmission indicated in Kenyan highlands
1998	Lindblade et al. (1999)	Epidemic starts in February in Ugandan highlands, authors associate outbreak with rainfall anomalies.
1998	Githeko and Ndegwa (2001)	Epidemic in Kenya from February 1998, but high incidence also reported in June/July 1997.
1998	Jones et al. (2007)	Epidemic in Tanzania highlands from February-June 1998, and high incidence also reported in summer of 1997.
2002	Hay et al. (2003)	Epidemic identified in Nandi and Kericho in June/July, with conditions returning to normal in August. Normal transmission occurred in Kisii and Gucha districts.
2005	Cox et al. (2007)	Examines DHIS data from 2002 to 2006 for Kabale and identifies outbreaks in 2005 (timing not described) and 2006 (centered on June) but questions the authenticity of the latter outbreak using confirmed data from a sentinel site.
2010	Ototo et al. (2011)	Report vector densities over period 09/2009 to 04/2010, reporting peak vector densities in Jan/Feb 2010. No long term dataset available to determine if conditions were anomalous.
2010	Yeka et al. (2012)	Describes general transmission in Uganda. Smear positivity rates for children under 5 show relative peak in Kanungu district (Kihihi) for Oct-Dec 2009 and May-July 2010 (their Fig. 4). No anomalies in selected high transmission zones.

Examining first the shorter range predictions one month in advance (Fig. 3 left column), encouragingly, there is model skill in malaria predictions in the target prediction zones throughout the calendar year. In some regions the predictability derives from correctly forecasting variations in temperature, but in southern Africa in a band stretching from Botswana through to Malawi and also across eastern Africa there are wide areas in which malaria predictive skill derives from both rainfall and temperature; for these the analysis does not show which variable contributes most to the skillful malaria prediction. In these regions rainfall predictability tends to be higher owing to stronger teleconnections with the El Niño phenomenon (Ropelewski and Halpert, 1987). Outside of these regions, skill in precipitation prediction appears limited in the areas of interest for malaria forecasting, in broad agreement with studies using the predecessor of the seasonal forecast (system 3) (Tompkins and Feudale, 2010; Vellinga et al., 2012). This is confirmed in the analysis of the first month rainfall skill compared to satellite retrievals conducted in the appendix.

In some locations the malaria forecasts are not significantly skillful, marked by a limited number of black points where predictions of all variables fail, or by blue, purple or red points which indicate skill in climate but not malaria prediction. In the northern-most Sahel belt spanning Senegal, Mali and Niger in July and August, wide
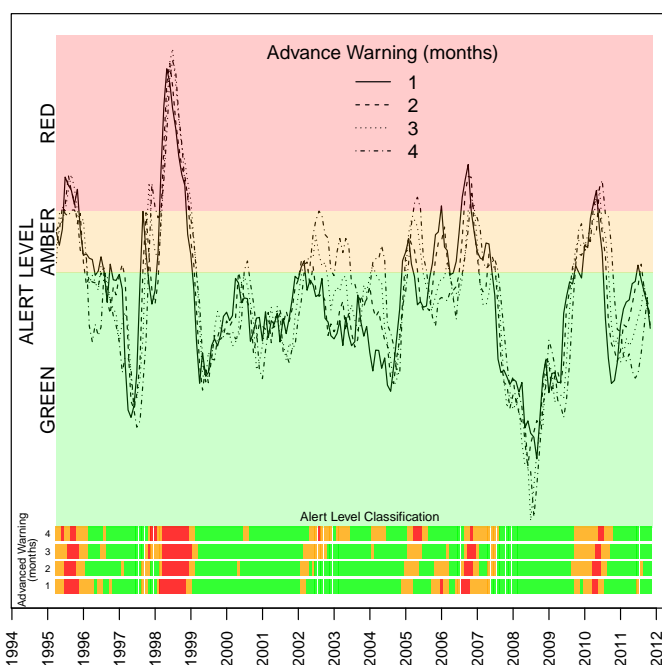
Figure 2. Timeseries of ensemble mean normalized forecasts of the natural logarithm of the EIR averaged for altitudes exceeding 1500m in the highlands of Uganda and Kenya with the annual cycle subtracted. Advance warnings (forecast lead time) of 1 to 4 months are shown. For example, the 4 month advance warning for June 2000 corresponds to a forecast that would be initialized at the beginning of March and issued shortly after, the issuing delay due to the time necessary to run the forecast system and post-process the results. A running mean is applied of 5 months to smooth the alert levels. For illustrative purposes the timeseries are nominally classified according to their mean percentile categories, with amber signifying an upper tercile event and red a 90th percentile occurrence. The colored boxes below the plot indicate the indicative warning level that might be communicated to a decision maker at these 4 different advance warning lead times.

areas display skill in temperature only (red colors) while in some points rainfall is also correctly predicted (purple colors) but no potential malaria prediction skill ensues. In this northern-most zone of the Sahel, rainfall variability and the northern extent of the monsoon limit malaria transmission (Thomson et al., 2004). Thus where rainfall predictions are inaccurate, a frequent short-coming in atmospheric models (Roehrig et al., 2013), malaria predictions will also fail. Where both rainfall and temperature are skillfully predicted, the failure to translate this into accurate malaria prediction could relate to the nonlinear relationship between transmission and rainfall, where intense rain events flush early stage larvae breeding sites (Paaijmans et al., 2007) and monsoon breaks lead to puddle desiccation (Gianotti et al., 2009). This nonlinearity is fully sampled by the high day-to-day variability of rainfall in the tropics, thus significant skill in predicting seasonal rainfall anomalies may not be sufficient if sub-seasonal rainfall variability is poorly represented.
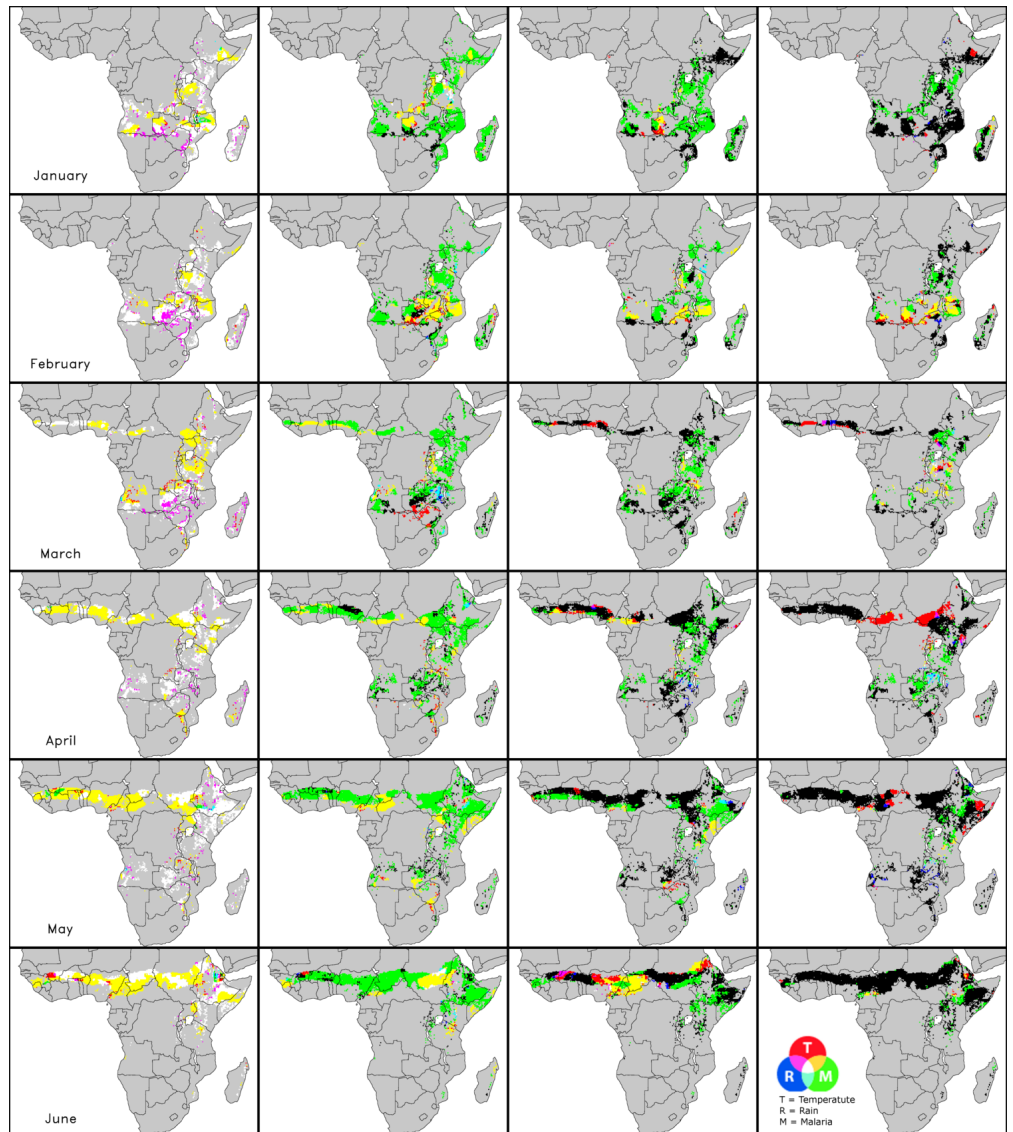
Figure 3. Composite plot of temperature (red), precipitation (blue) and malaria (ln(EIR), green) forecast anomaly correlation coefficients that are statistically skillful at the 95% confidence level for issuing warnings for 1 through 4 months in advance (lead time) for each calendar month of the year. White points mark cells with skill in all three variables, black points mark cells without any skill. See legend for color definitions of intersecting categories. (CONTINUED)

Analyzing the potential malaria prediction skill for longer lead times of two to four months (Fig. 3, columns 2 to 4), it is seen that the climate prediction system exhibits a sharp drop in skill at predicting rainfall and temperature two months in advance compared to one month. Despite this, there are wide areas for which the pilot MEWS still has significant skill for malaria prediction in months 2 and 3, and in smaller regions even four months ahead. This is due to the inherent lags between the rainfall anomalies and the resulting malaria transmission season, such that the skill in predicting malaria transmission in the second and third month derives from the climate information contained in the forecast initial conditions and the first month forecast of climate. This
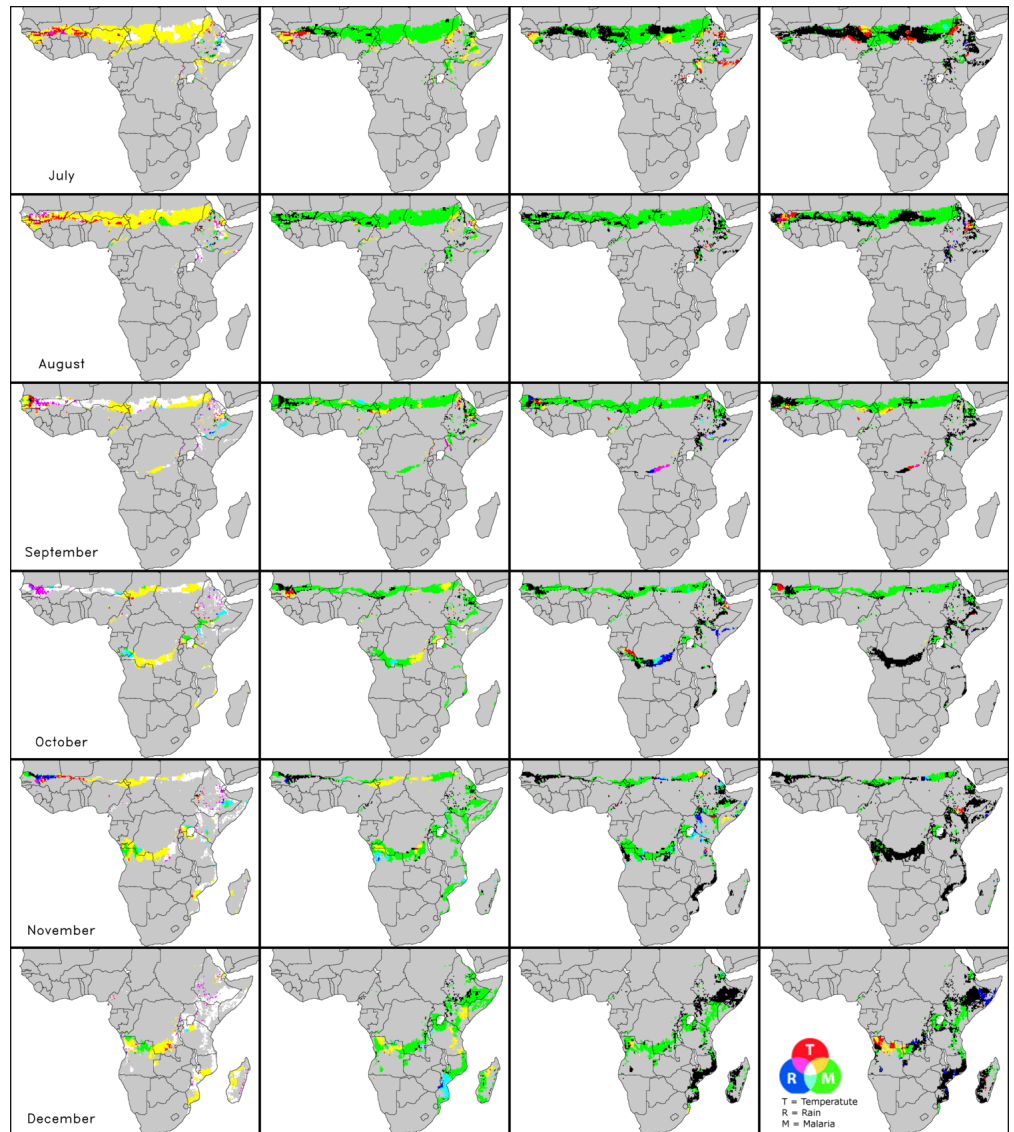
Figure 3. cont.

highlights the crucial role that the malaria analysis system has in correctly initializing the malaria modelling system. In areas where rainfall and temperatures are predictable beyond one month, such as in Eastern Africa, the malaria prediction advanced warning is extended beyond the 3 month range. The analysis thus indicates that by driving the malaria model with dynamical climate forecasts, useful information regarding the future transmission season in epidemic and seasonally variable endemic regions can potentially be delivered at least one, and in limited regions, two to three months earlier than would otherwise be the case using climate observations, which themselves provide more advance warning than the direct monitoring of symptomatic malaria cases (Thomson et al., 2006).

We have also extensively examined the prediction skill of malaria in the highlands of Uganda. Preliminary results are reported in Tompkins et al. (2016a) (Refer to case study 5.J on page 130, link in reference list). A preliminary version of the system was

tested in Rwanda, (Fig. 4) and was found to have skill at a lead time of 4 months in the west and south of the country, but unfortunately not in the eastern regions, which are some of the districts with the highest prevalence. Further examination of the forecast skill of a newer version of the system applied to Uganda can not yet be reported in detail here as the aim is to submit the work to Nature which precludes pre-publication of information online. These will be made available after the result of the review process is known.

Entomological Inoculation Rate
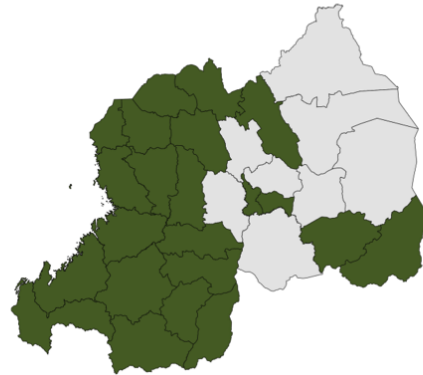### *Areas with skill*

Figure 4. Districts in Rwanda in which the ECMWF-ICTP forecast system has significant skill at a lead time of 4 months

Finally, the uncertainty of the malaria forecasting system is not accounted for in the forecasting system presented here. The ensemble members only account for differences due to the driving climate and climatic initial conditions. In the third year of the project, preliminary tests were conducted at incorporating a perturbed-parameter ensemble for the malaria model (An example for a location in Uganda is given in Fig. 5, taken from Tompkins et al. (2016b)) which showed the considerable potential uncertainty due to the malaria model parameter settings, particularly in highland settings close to the onset temperature threshold. This work has lead to the development of a new genetic calibration algorithm for ensemble integrations in the follow on project.

Conclusions

The EPS and SYS4 systems have been successfully coupled to the VECTRI malaria model as planned during the period of the project. The system has been extensively validated in Rwanda, Uganda, Tanzania and Malawi and skill proven at predicting outbreaks, particularly in highland areas. The project has lead to a large number of publications detailed below. The aim is now to attempt to interface the system with public health policy in Uganda and work towards a pre-operational pilot implementation during 2017-2018.

Entomological Inoculation Rate
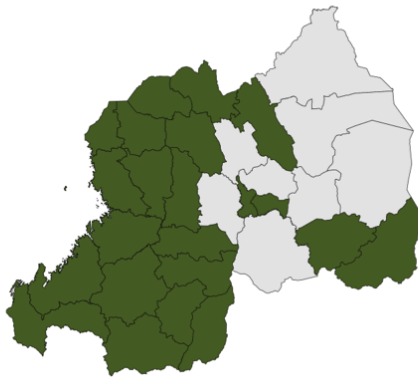### *Areas with skill*

Figure 5. 60 member ensemble integrations for Mbarara in Uganda

APPENDIX: IFS developments for the Radiation scheme

Although not directly related to the health topic, while investigating the factors affecting the two metre temperature over Africa, the radiation code was examined in detail and a number of issues were identified as reported in the SPITP4DC third annual report. As stated in that report, the aim was to resolve these issues and pass a documented branch to ECMWF with these IFS code contributions. This Appendix contains a copy of the branch report to retain a record of these IFS developments that occurred within SPITP4DC. The issues identified are mostly related to the way cloud overlap is parameterized in the model.

The assumption of how clouds overlap in the vertical is still today one of the key factors determining differences between atmospheric model radiation schemes (Zhang et al., 2013). The long-standing de facto assumption implemented in models has been the so-called MAX-RAN scheme. This applies diverse assumptions depending on whether clouds are present in continuous layers, or whether clouds are separated by clear sky layers (referred to hereafter as non-continuous clouds). Contiguous clouds were assumed to be maximally overlapped, while clouds separated by a clear sky layer are instead assumed to be randomly overlapped Morcrette and Fouquart (1986)

A number of modelling and observational studies showed that, while a reasonable representation of observed cloud statistics, the MAX-RAN assumption tended to underestimate total cloud cover, since clouds continuously present in through many layers tended to decorrelate as the layer separation increased, due to the effects of horizontal wind shear for example. Hogan and Illingworth (2000) (hereafter HI00) thus suggested a simple modification to the MAX-RAN scheme whereby the overlap of clouds was given by a parameter α, which describes the overlap in terms of a linear mix between the RAN and MAX assumptions.

HI00 suggested that at small layer separations in contiguous clouds α should be close to unity for maximum overlap, but that it would decrease towards zero as the layer separation increased and the cloud in the layers became decorrelated. By fitting an exponential curve to observations of α as a function of layer separation distance, HI00 derived the decorrelation length scale L for contiguous clouds to be around 2 km for the ground-based observations taken over southern England. The data also supported the assumption of random overlap for layers separated by a clear sky gap in the vertical. The resulting scheme was coined the EXP-RAN scheme by Tompkins and Di Giuseppe

(2007) as continuous clouds exponentially decorrelate, and non-continuous clouds are randomly overlapped.

Although the actual value for L determined from observations varies substantially as a function of cloud dynamics, horizontal wind shear (Mace and Benson-Troth, 2002; Hogan and Illingworth, 2003; Naud et al., 2008; Mace et al., 2009; Oreopoulos and Norris, 2011; Di Giuseppe and Tompkins, 2015), location (Shonk et al., 2010; Oreopoulos and Norris, 2011) and even the analysis method itself (Tompkins and Di Giuseppe, 2015a), the underlying validity of the EXP-RAN approach has been widely confirmed. There does, however, exist an alternative simpler approach, which was advocated by Barker et al. (2008) and implemented in the scheme of Bergman and Rasch (2002). This approach simplifies the EXP-RAN scheme by simply assuming a fixed decorrelation length scale for all cloud situations, both continuous and non-continuous. This approach has the advantage of simplicity but is less supported by observations.

In common with a number of models, the ECMWF radiation schemes for short-wave and long-wave radiation transfer now externalize the overlap assumption by the implementation of what is known the the Monte Carlo Independent Column Approximation (McICA) approach (Pincus et al., 2003; Räisänen et al., 2005; Morcrette et al., 2008). In this method, the vertical profile of cloud fraction in each column is randomly sampled to generate a number of potential sub-columns, in which each layer is either cloud-free or overcast (Pincus et al., 2003; Räisänen et al., 2005; Morcrette et al., 2008). Each g-point calculation of the radiation scheme is performed using one of these randomly-sampled columns. Averaged over many sub-columns, the cloud fraction profile of the ECMWF grid column will be obtained, within the expected tolerance according to the sample size. The overlap assumption is therefore moved outside of the radiation scheme to the so-called cloud generator, improving simplicity and efficiency of the radiation calculation.

The implementation of the overlap assumption has a number of issues, however. The overlap assumption used is not clearly stated, and the online IFS documentation is actually incorrect, and has been so for the past 8 years, indicating the radiation scheme's authors at ECMWF were also unaware of which overlap scheme was actually encoded in the Räisänen et al. (2004) algorithm employed in the IFS. Moreover there are a number of other issues concerning performance and accuracy of the code. The aim of this report is to briefly outline these and then introduce a branch that addresses the main shortcomings.

Issues with the IFS

The key issues concerning the IFS are:

1. Contrary to popular belief (and the IFS online documentation!) the overlap assumption employed by the radiation scheme is **not** the EXP-RAN scheme of Hogan and Illingworth (2000), but rather a simpler scheme that assume EXP overlap for all clouds, irrespective of whether or not they are separately by clear sky gaps

2. The random numbers are not truly random as they are seeded every timestep (bad idea) and the choice of seed is poor.

3. Due to the way the random number vectors are initialized, the overlap scheme has all the loops in an inverted order, leading to severe performance issues in a routine that is computationally intensive (i.e. many column calculations per radiation grid-point).

4. The (optional) MAX-RAN overlap assumption is coded using an inferior algorithm which is inconsistent with algorithm used for the EXP-RAN overlap and is also highly vertical resolution sensitive.

The above issues are described in more detail in this section, while the subsequent section introduces branches that corrects issues 1, 3 and 4, tidies up some of the code, converts some previously hard-wired constants to variables that are set in the radiation namelists for flexibility and introduces an optional implementation of the wind-shear dependent overlap scheme.

IFS Overlap assumption is EXP and not EXP-RAN

One of the key issues is not a coding bug per-se, but is a issue regarding a general misunderstanding of which overlap schemed the IFS actually employs. To generate the sub-columns, the ECMWF IFS implements the overlap algorithms of Räisänen et al. (2004). In Räisänen et al. (2004), two algorithms are described, the first referred to as *generalized overlap* assumption, which is the default option in the IFS. The paper then also introduces a revised algorithm for the MAX-RAN overlap. When referring to the generalized overlap, Räisänen et al. (2004) cites two studies: Hogan and Illingworth (2000) and Bergman and Rasch (2002), but without discussing the specifics of the overlap assumptions. This is unfortunate, since Hogan and Illingworth (2000) and Bergman and Rasch (2002) describe two related, but very distinct schemes.

Thus, the reader must interpret the algorithm of Räisänen et al. (2004) to understand which of the two schemes has been employed. This has lead to some confusion, and it is notable that most studies that discuss the radiation scheme of the ECMWF IFS either never mention overlap at all, or merely refer to the assumption as generalized overlap and cite the implementation description of Morcrette et al. (2008). For example, Troccoli and Morcrette (2014) uses short wave radiation statistics of the IFS in a study but avoids discussing the overlap specifics.

Most importantly, the IFS online documentation itself greatly exacerbates this confusion, since when it discusses the details of the overlap scheme employed, it *only* refers to the EXP-RAN scheme of Hogan and Illingworth (2000) and neglects to mention the EXP scheme of Bergman and Rasch (2002) at all, giving the impression to the reader that even ECMWF itself believes that the EXP-RAN scheme is used in the model.

It is straightforward to add a minor modification to the generator algorithm in order to change the EXP assumption to EXP-RAN by adding a condition to the formula given in equation 9 of Räisänen et al. (2004). The original formula was given as

$$x_{j,k} = \begin{cases} x_{j,k-1} & \text{for } RN2_{j,k} \leq \alpha_{j-1,k}, \\ RN3_{j,k} & \text{for } RN2_{j,k} > \alpha_{j-1,k}. \end{cases}$$

where RN2 and RN3 represent independent random number streams, and $x_{j,k} \in [0,1]$ is used to determine whether a cell is cloudy or clear (see their equation 1). The decorrelation length-scale of clouds determines the parameter α. The reader is referred to Hogan and Illingworth (2000) and Räisänen et al. (2004) for further details. This can be modified to model EXP-RAN very easily by simply adding a further condition

$$x_{j,k} = \begin{cases} RN3_{j,k} & \text{for } RN2_{j,k} > \alpha_{j-1,k} \text{ OR } C_{j,k-1} = 0, \\ x_{j,k-1} & \text{otherwise .} \end{cases}$$

Note the use of random number stream RN1 Räisänen et al. (2004) to initialize $x_{j,k}$ at the top of the cloud layer was redundant and confuses the interpretation of the scheme logic. One can simply set $x_{j,1} = RN2_{j,1}$ removing the need to initialize RN1.

Random numbers

The second issue of the scheme is that the random number generation methodology is poorly implemented. The random number vectors for each radiation gridpoint are seeded *every timestep*. This is usually strongly advised against as it makes the numbers not truly random. Moreover, the recipe for the seed uses an additive formula, combining latitude, longitude and time:

$$seed = NINT(PGLON(IL) + PGLAT(IL) + ITIM + IDAY) \qquad (1)$$

By adding longitude and latitude indices in this way, it is clear that many gridpoints share the same seed value on a given timestep, and indeed values are shared with nearby columns on subsequent timesteps. This results identical random vectors being used for many columns. From a brief investigation, it was estimated that a 24 hour forecast uses a mere $O(10^3)$ independent random number streams. This would be the same even at the highest resolution, since the latitude and longitude values are simply rounded to the nearest integer after summing.

 The impact of this effect was tested briefly against a branch in which all columns are seeded with a unique number only once at the integration start, and the impact is limited. The solution is not adequate for implementation however as it would not be bit-reproducible. The random number vectors should rather be initialized at the integration outset by mimicking the method used in the stochastic physics routines.

Performance issues

In addition the previous code had a number of performance and clarity issues. The code generated three vectors of random numbers, where only two are actually used in the algorithm implementation, which no only slows the code slightly, but also confuses the code substantially and makes its understanding much more involved. In addition, some legacy code lines were effectively redundant and have been removed or cleaned up.

 Much more importantly for performance, due to the way the random number vectors were generated, all the nested do-loops are inverted, which would significantly affect routine performance by an order of magnitude. In the branch made available, all do loops are written in storage-order and the routine should now be an order of magnitude faster.

IFS code reordering

A brief note on MAX-RAN

The generator of Räisänen et al. (2004) also implements and algorithm for the MAX-RAN overlap scheme, which is also included in the IFS as a non-default option under a switch. The algorithm implements a local pair-wise implementation of the MAX-RAN overlap, which is undesirable as it is subject to considerable vertical resolution sensitivities, as discussed by Tompkins and Di Giuseppe (2015b). This is in contrast to the EXP-RAN implementation which uses a more robust and correct, non-local overlap implementation. The result is that continuous cloudy layers also decorrelate in the MAX-RAN scheme, with the decorrelation length-scale a function of the model vertical resolution. This choice is somewhat bizarre, as Räisänen et al. (2004) correctly notes after eqn 9 that MAX overlap is simply a special case of the EXP overlap, but then implements the different algorithm for MAX-RAN in eqn 14. This is presumably because he has chosen to implement the EXP rather than the EXP-RAN scheme, since if the latter had been coded, the MAX-RAN scheme is a trivial special case.

Table 2. IFS Switches

Switch	Previous	New
NDECOLAT (overlap control)	0=fixed decorrelation length (set by RDECORR_CF and RDECORR_CW), 1=Shonk et al. (2010) latitude scheme, 2=modified Shonk	3=Wind shear dependence set using RDECORR_CF + $d\mathcal{W}/dz$ RDECORR_CF_WS
LPPH (plane parallel clouds)	was hardwired within code to true for MAX-RAN and false for EXP	now set by namelist, default value is FALSE to maintain default set up.
LPOLICE (ice effective radius at poles)	was a fixed value in code	now a parameter set in a namelist, default value unchanged

The opportunity was taken to modify the algorithm to use a consistent approach for both EXP-RAN and MAX-RAN options. MAX-RAN is now a special case of EXP-RAN simply, which implies the MAX-RAN scheme now gives the identical answer to the EXP-RAN scheme as $L \to \infty$. For details of the algorithmic change refer to Tompkins and Di Giuseppe (2015b). This also greatly simplifies the logic of the scheme.

Wind shear dependent overlap

The branches below include code for the new wind shear dependent overlap scheme outlined in Di Giuseppe and Tompkins (2015). Thus there are a considerable number of routines that have been modified in order to pass the wind fields through the interpolation routines to the radiation grid. Details of the implementation are given in the branch overview below.

Implementation

switches

In the new branch described below, a number of new switches/options have been added, see table 2.

branch

Branch *client_cpa_CY41R1_wind_shear_overlap_expran* is a start point for further testing and development. In addition to addressing some of the issues above, the branch also implements the wind-shear dependent overlap of Di Giuseppe and Tompkins (2015) under a switch (NDECOLAT=3, but the default value is still set to 2 for the modified Shonk latitude-dependency scheme). In order to implement this, a considerable number of routines required minor configuration changes to enable the passing of the wind fields to the radiation routine. An overview of the branch is given in table 3.

IFS integrations

Tests conducted on these branches use a setup consisting of 2 weeks of 24 hour forecasts performed at T95/L91 resolution. Short, 24 hour, integrations allow one to discern the impact of the overlap assumption on the radiation budgets without the complication of cloud-radiative feedback effects on the dynamics and the experiment resolution was

Table 3. Overview of IFS Branch client_cpa_CY41R1_wind_shear_overlap_expran

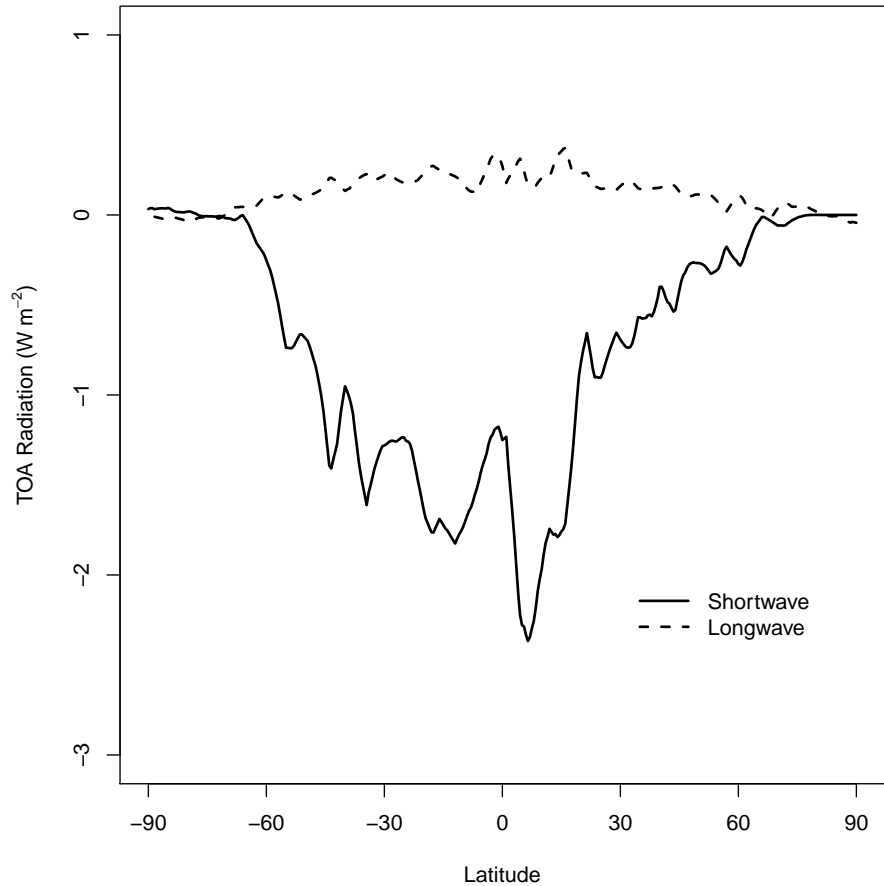|	
module/ yoecld.F90	RDECORR_CF and RDECORR_CW deleted (moved to yoerad.F90)
module/ yoerad.F90	RDECORR_CF and RDECORR_CW moved here for consistency, and
	RDECORR_CF_WS and RDECORR_CF_WS add to control the wind-shear dependent overlap parameterization of Di Giuseppe and Tompkins (2015)
	RPOLICE added : Ice effective radius in microns at poles (previously hardwired).
	LPPH added
namelist/	RDECORR_CF,RDECORR_CW,
naerad.nam.h	RDECORR_CF_WS, RDECORR_CW_WS, LPPH added.
	NOTE: LPPH is now set independently of the choice of EXP-RAN or MAX-RAN, the default options have not changed.
phys_dmn/ surdi15.F90	Compatibility changes in legacy code
phys_ec/ callparad.F90	Compatibility changes for wind passing
phys_ec/ cldpp.F90	Compatibility changes for wind passing
phys_ec/ cldprg_layer.F90	Changes to pass down winds to radiation schemes
phys_ec/ raddrv.F90	Changes to pass down winds to radiation schemes
phys_ec/ radiation_layer.F90	Changes to pass down winds to radiation schemes
phys_ec/ radina.F90	Changes to pass down winds to radiation schemes
phys_ec/ radintg.F90	Changes to pass down winds to radiation schemes
phys_ec/ radlswr.F90	added wind-shear parameterization for alpha overlap (NDECOLAT=3)
	added RPOLICE for case NMINICE=1 to generalize parameterization
	removed local definition of LPPH - now set in module
phys_ec/ radpar.F90	Changes to pass down winds to radiation schemes
phys_ec/ sucld.F90	Set default values for new parameters
phys_radi/ mcica_cld_gen.F90	removed LPPH from interface to cloud generator as it is now in module YOERAD
phys_radi/ mcica_cld_generator.F90	Changed EXP overlap assumption to EXP-RAN
	Corrected optional MAX-RAN overlap to be correct and consistent with EXP-RAN approach rather than using the pair-wise overlap as previously
	Reversed JL,JK loops to make code much more efficient and tidied up code.
	NOTE: random_number generator not changed, but needs attention. seeding should only be done first timestep and the seed is poorly chosen so that there are a lot of grid-columns using the same values.
	LPPH read from module YOERAD
phys_radi/ suecrad.F90	default values set for RPOLICE=20 RDECORR_CF=2.0 RDECORR_CW = 1.0 RDECORR_CF_WS = 0.35 RDECORR_CW_WS = 0.35 LPPH=.FALSE.

Figure 6. Difference between the time averaged zonal mean shortwave (upper) and longwave (lower) radiative fluxes between using the EXP-RAN scheme of Hogan and Illingworth (2000) instead of the (present default) EXP scheme of Bergman and Rasch (2002)

designed to be computationally economical to be run using a member state unit allocation. A full list of experiment identifiers is available on request.

As an example Fig. 6 shows the mean impact of the implementing the EXP-RAN scheme versus the EXP overlap scheme, in this case using a constant $L = 3km$ but there are also experiments using the alternative options. For the short wave calculation it is seen that the impact is on the order of 2 W m^{-2}. This is comparable to the impact of switching the overlap parametrization from fixed 3km decorrelation length-scale to the latitude-dependent scheme of Shonk et al. (2010) or the wind-shear scheme of Di Giuseppe and Tompkins (2015) (see Fig. 7 which is reproduced from Di Giuseppe and Tompkins (2015).

Summary of Appendix

In summary, a branch has been presented that has the following attributes:

1. The overlap assumption has been changed from a simple EXP scheme to the EXP-RAN scheme of Hogan and Illingworth (2000), which more accurately describes the observed statistics of cloud overlap in observations.
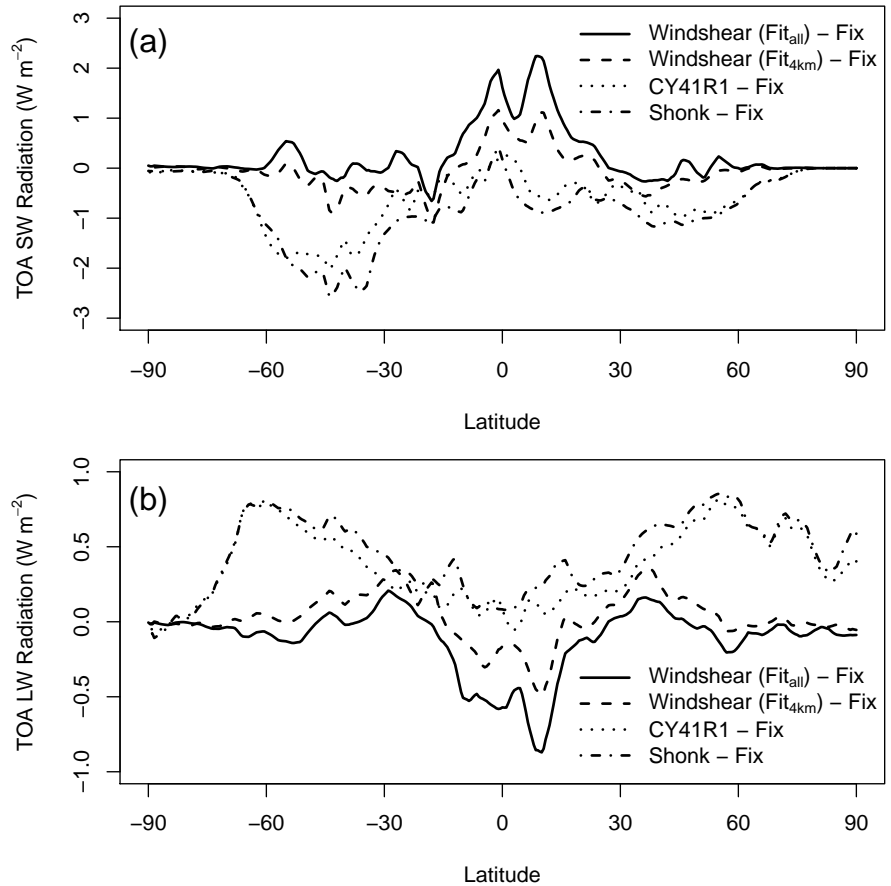
Figure 7. Zonal average differences of top of atmosphere (TOA) (a) shortwave (SW) and (b) longwave (LW) fluxes between the Shonk, CY41R1, wind shear parameterizations with respect to the fixed decorrelation lengthscale of 3 km (Fix), defined in the legend. Positive values indicate an increase in the downward direction. Figure reproduced from Di Giuseppe and Tompkins (2015)

2. The loop order has been changed in the cloud sub-column generator code and superfluous random number vectors have been removed. Together these changes should decrease the CPU time of this routine by approximately an order of magnitude, which is important as this is a heavy part of the code generating $O(10^2)$ sub-columns for each radiative gridpoint.

3. The (optional) MAX-RAN overlap assumption is now coded to be self-consistent with the EXP-RAN assumption and is no longer sensitive to the vertical resolution selected.

4. An additional decorrelation length-scale parameterization scheme has been added which parametrizes the decorrelation as a function of wind-shear according to Di Giuseppe and Tompkins (2015). Set NDECOLAT=3 to select this scheme (default value is NDECOLAT=2). This implementation involves a slight computational overhead even if the scheme is not selected due to the fact that the winds need to be passed down to the level of the radiation calculations, which is done whether or not the scheme is selected.

5. The plane parallel assumption is no longer selected according to the choice of

EXP or MAX-RAN, but is now an independent parameter. The default setting is LPPH=FALSE to maintain consistency with the present operational configuration.

6. LPPH, RPOLICE and the new overlap parameters for the wind shear parametrization RDECORR_CF_WS and RDECORR_CW_WS and now definable in the radiation namelist.

References

Alonso, D., M. J. Bouma, and M. Pascual, 2011: Epidemic malaria and warmer temperatures in recent decades in an East African highland. *Proc R Soc Lond B Biol Sci*, **278**, 1661–1669.

Barker, H. W., J. N. S. Cole, J. J. Morcrette, R. Pincus, P. Räisänen, K. von Salzen, and P. A. Vaillancourt, 2008: The Monte Carlo Independent Column Approximation: an assessment using several global atmospheric models. *Q. J. R. Meteorol. Soc.*, **134**, 1463–1478.

Bergman, J. W., and P. J. Rasch, 2002: Parameterizing vertically coherent cloud distributions. *J. Atmos. Sci.*, **59**, 2165–2182.

Cox, J., S. I. Hay, T. A. Abeku, F. Checchi, and R. W. Snow, 2007: The uncertain burden of *Plasmodium falciparum* epidemics in Africa. *Trends Parasitol*, **23 (4)**, 142–148.

Dee, D. P., and Coauthors, 2011: The ERA-Interim reanalysis: configuration and performance of the data assimilation system. *Q. J. R. Meteorol. Soc.*, **137 (656)**, 553–597.

Di Giuseppe, F., and A. M. Tompkins, 2015: Generalizing cloud overlap treatment to include the effect of wind shear. *J. Atmos. Sci.*, **72**, 2865–2876.

Diro, G. T., A. M. Tompkins, and X. Bi, 2012: Dynamical downscaling of ECMWF ensemble seasonal forecasts over East Africa with RegCM3. *J. Geophys. Res.*, **117 (D16)**, doi: 10.1029/2011JD016 997.

Dutra, E., F. Di Giuseppe, F. Wetterhall, and F. Pappenberger, 2013: Seasonal forecasts of droughts in african basins using the standardized precipitation index. *Hydrology and Earth System Sciences*, **17 (6)**, 2359–2373.

Gianotti, R. L., A. Bomblies, and E. A. B. Eltahir, 2009: Hydrologic modeling to screen potential environmental management methods for malaria vector control in Niger. *Water Resour Res*, **45**, W08 438, doi:10.1029/2008WR007 567.

Giorgi, F., R. Francisco, and J. Pal, 2003: Effects of a subgrid-scale topography and land use scheme on the simulation of surface climate and hydrology. Part I: Effects of temperature and water vapor disaggregation. *J. Hydrometeor.*, **4**, 317–333.

Githeko, A. K., and W. Ndegwa, 2001: Predicting malaria epidemics in the Kenyan highlands using climate data: a tool for decision makers. *Glob Chan Hum Health*, **2**, 54–63.

Hay, S. I., M. Renshaw, S. A. Ochola, A. M. Noor, and R. W. Snow, 2003: Performance of forecasting, warning and detection of malaria epidemics in the highlands of western Kenya. *Trends Parasitol*, **19**, 394–399.

Hogan, R. J., and A. J. Illingworth, 2000: Deriving cloud overlap statistics from radar. *Q. J. R. Meteorol. Soc.*, **126**, 2903–2909.

Hogan, R. J., and A. J. Illingworth, 2003: Parameterizing ice cloud inhomogeneity and the overlap of inhomogeneities using cloud radar data. *J. Atmos. Sci.*, **60**, 756–767.

Jones, A. E., U. U. Wort, A. P. Morse, I. M. Hastings, and A. S. Gagnon, 2007: Climate prediction of El Niño malaria epidemics in north-west Tanzania. *Malar J*, **6 (1)**, doi:10.1186/1475–2875–6–162.

Jones, P. W., 1999: First-and second-order conservative remapping schemes for grids in spherical coordinates. *Mon. Wea. Rev.*, **127 (9)**, 2204–2210.

Lindblade, K. A., E. D. Walker, A. W. Onapa, J. Katungu, and M. L. Wilson, 1999: Highland malaria in Uganda: prospective analysis of an epidemic associated with El Niño. *Trans R Soc Trop Med Hyg*, **93 (5)**, 480–487.

Mabaso, M. L. H., and N. C. Ndlovu, 2012: Critical review of research literature on climate-driven malaria epidemics in sub-Saharan Africa. *Public Health*, **126 (11)**, 909–919.

Mace, G. G., and S. Benson-Troth, 2002: Cloud-layer overlap characteristics derived from long-term cloud radar data. *J. Climate*, **15**, 2505–2515.

Mace, G. G., Q. Zhang, M. Vaughan, R. Marchand, G. Stephens, C. Trepte, and D. Winker, 2009: A description of hydrometeor layer occurrence statistics derived from the first year of merged CloudSat and CALIPSO data. *J. Geophys. Res.*, **114**, DOI: 10.1029/2007JD009 755.

Molteni, F., and Coauthors, 2011: The new ECMWF seasonal forecast system (System 4). Tech. rep., European Centre for Medium-Range Weather Forecasts, available at http://www.ecmwf.int/publications, 656:51 pp.

Morcrette, J., H. Barker, J. Cole, M. Iacono, and R. Pincus, 2008: Impact of a new radiation package, McRad, in the ECMWF Integrated Forecasting System. *Mon. Wea. Rev.*, **136 (12)**, 4773–4798.

Morcrette, J.-J., and Y. Fouquart, 1986: The overlapping of cloud layers in shortwave radiation parameterizations. *J. Atmos. Sci.*, **43**, 321–328.

Murphy, A. H., and E. S. Epstein, 1989: Skill scores and correlation coefficients in model verification. *Mon. Wea. Rev.*, **117**, 572–582.

Naud, C. M., A. Del Genio, G. G. Mace, S. Benson, E. E. Clothiaux, and P. Kollias, 2008: Impact of dynamics and atmospheric state on cloud vertical overlap. *J. Climate*, **21 (8)**, 1758–1770.

Oreopoulos, L., and P. Norris, 2011: An analysis of cloud overlap at a midlatitude atmospheric observation facility. *Atmos. Chem. Phys.*, **11 (12)**, 5557–5567.

Ototo, E. N., A. K. Githeko, C. L. Wanjala, and T. W. Scott, 2011: Surveillance of vector populations and malaria transmission during the 2009/10 El Niño event in the western Kenya highlands: opportunities for early detection of malaria hyper-transmission. *Parasit Vectors*, **4**, 144.

Paaijmans, K. P., M. O. Wandago, A. K. Githeko, and W. Takken, 2007: Unexpected high losses of Anopheles gambiae larvae due to rainfall. *PLoS ONE*, **2**, e1146, doi:10.1371/journal.pone.0001 146.

Pincus, R., H. W. Barker, and J. J. Morcrette, 2003: A fast, flexible, approximate technique for computing radiative transfer in inhomogeneous cloud fields. *J. Geophys. Res.*, **108**, 10.1029/2002JD003 322.

Räisänen, P., H. W. Barker, and J. N. S. Cole, 2005: The Monte Carlo independent column approximation's conditional random noise: impact on simulated climate. *J. Climate*, **18**, 4715–4730.

Räisänen, P., H. W. Barker, M. F. Khairoutdinov, J. Li, and D. A. Randall, 2004: Stochastic generation of subgrid-scale cloudy columns for large-scale models. *Q. J. R. Meteorol. Soc.*, **130 (601)**, 2047–2067.

Roehrig, R., D. Bouniol, F. Guichard, F. Hourdin, and J.-L. Redelsperger, 2013: The present and future of the West African monsoon: a process-oriented assessment of CMIP5 simulations along the AMMA transect. *J. Climate*, **26**, 6471–6505.

Ropelewski, C. F., and M. S. Halpert, 1987: Global and regional scale precipitation patterns associated with El Niño/Southern Oscillation. *Mon. Wea. Rev.*, **115**, 1606–1626.

Shonk, J. K., R. J. Hogan, J. M. Edwards, and G. G. Mace, 2010: Effect of improving representation of horizontal and vertical cloud structure on the earth's global radiation budget. part i: Review and parametrization. *Q. J. R. Meteorol. Soc.*, **136 (650)**, 1191–1204.

Thiemig, V., R. Rojas, M. Zambrano-Bigiarini, V. Levizzani, and A. De Roo, 2012: Validation of satellite-based precipitation products over sparsely gauged african river basins. *J. Hydrometeor.*, **13 (6)**, 1760–1783.

Thomson, M. C., S. J. Connor, N. Ward, and D. Molyneux, 2004: Impact of climate variability on infectious disease in West Africa. *Ecohealth*, **1 (2)**, 138–150.

Thomson, M. C., F. J. Doblas-Reyes, S. J. Mason, R. Hagedorn, S. J. Connor, T. Phindela, A. P. Morse, and T. N. Palmer, 2006: Malaria early warnings based on seasonal climate forecasts from multi-model ensembles. *Nature*, **439**, 576–579.

Tompkins, A. M., and F. Di Giuseppe, 2007: Generalizing cloud overlap treatment to include solar zenith angle effects on cloud geometry. *J. Atmos. Sci.*, **64**, 2116–2125.

Tompkins, A. M., and F. Di Giuseppe, 2015a: An interpretation of cloud overlap statistics. *J. Atmos. Sci.*, **72**, 2877–2889, URL http://journals.ametsoc.org/doi/abs/10.1175/JAS-D-14-0278.1.

Tompkins, A. M., and F. Di Giuseppe, 2015b: Potential predictability of malaria using ECMWF monthly and seasonal climate forecasts in Africa. *J. Appl. Meteor. Clim*, **54**, 521–540, URL http://journals.ametsoc.org/doi/abs/10.1175/JAMC-D-14-0156.1.

Tompkins, A. M., F. Di Giuseppe, F. J. Colón-González, and D. B. Namanya, 2016a: A planned operational malaria early warning system for Uganda provides useful district-scale predictions up to 4 months ahead. *Climate services for health: Case studies of enhancing decision support for climate risk management and adaptation.*, J.Shumake-Guillemot, and L.Fernandez-Montoya, Eds., WHO/WMO Geneva, 130–131, URL http://ane4bf-datap1.s3-eu-west-1.amazonaws.com/wmocms/ s3fs-public/WHO-WMO_Case_Studies_draft_FULL_2.pdf? i3omNE2N2V7_nX1uYYg6bvqnaR1kiwMn.

Tompkins, A. M., and V. Ermert, 2013: A regional-scale, high resolution dynamical malaria model that accounts for population density, climate and surface hydrology. *Malaria Journal*, **12**, doi:10.1186/1475–2875–12–65, URL http://link.springer.com/article/10.1186/1475-2875-12-65.

Tompkins, A. M., and L. Feudale, 2010: West Africa monsoon seasonal precipitation forecasts in ECMWF System 3 with a focus on the AMMA SOP. *Wea. and Forecasting*, **25**, 768–788, URL http://journals.ametsoc.org/doi/abs/10.1175/2009WAF2222236.1.

Tompkins, A. M., L. Larsen, N. McCreesh, and D. M. Taylor, 2016b: To what extent does climate explain variations in reported malaria cases in early 20th century Uganda? *Geospat. Health*, **11**, 10.4081/gh.2016.407, URL http://geospatialhealth.net/index.php/gh/article/view/407.

Troccoli, A., and J.-J. Morcrette, 2014: Skill of direct solar radiation predicted by the ecmwf global atmospheric model over australia. *J. Appl. Meteor. Clim*, **53 (11)**, 2571–2588.

Vellinga, M., A. Arribas, and R. Graham, 2012: Seasonal forecasts for regional onset of the West African monsoon. *Climate Dynamics*, **40**, 1–24.

Vitart, F., and Coauthors, 2008: The new VarEPS-monthly forecasting system: A first step towards seamless prediction. *Q. J. R. Meteorol. Soc.*, **134 (636)**, 1789–1799.

Yeka, A., and Coauthors, 2012: Malaria in Uganda: challenges to control on the long road to elimination: I. Epidemiology and current control efforts. *Acta Trop*, **121 (3)**, 184–195.

Zhang, F., X.-Z. Liang, J. Li, and Q. Zeng, 2013: Dominant roles of subgrid-scale cloud structures in model diversity of cloud radiative effects. *J. Geophys. Res.*, **118 (14)**, 7733–7749.

List of publications/reports from the project with complete references

A. M. Tompkins, L. Larsen, N. McCreesh, and D. M. Taylor. To what extent does climate explain variations in reported malaria cases in early 20th century Uganda? Geospat. Health, 11:10.4081/gh.2016.407, 2016.

A. M. Tompkins and N. McCreesh. Migration statistics relevant for malaria transmission in Senegal derived from mobile phone data and used in an agent-based migration model. Geospat. Health, 11:doi:10.4081/gh.2016.408, 2016.

A. M. Tompkins, F. Di Giuseppe, F. J. Colon-González, and D. B. Namanya. A planned operational malaria early warning system for Uganda provides useful district-scale predictions up to 4 months ahead. In J.Shumake-Guillemot and L.Fernandez-Montoya, editors, Climate services for health: Case studies of enhancing decision support for climate risk management and adaptation. WHO/WMO Geneva, 2016.

Ernest O. Asare, Adrian M. Tompkins, Leonard K. Amekudzi, and Volker. Ermert. A breeding site model for regional, dynamical malaria simulations evaluated using in situ temporary ponds observations. Geospat. Health, 11:DOI: 10.4081/gh.2016.390, 2016.

Ernest O. Asare, Adrian M. Tompkins, Leonard K Amekudzi, Volker. Ermert, and Schuster R. Mosquito breeding site water temperature observations and simulations towards improved vector-borne disease models for Africa. Geospat. Health, 11:DOI: 10.4081/gh.2016.391, 2016. [http | http]

E. Asare, A. M. Tompkins, and A. Bomblies. Evaluation of a simple puddle breeding site model for malaria vectors using high resolution explicit surface hydrology simulations. PLoS ONE, 11:http://dx.doi.org/10.1371/journal.pone.0150626, 2016.

F. J. Colón-González, A. M. Tompkins, R. Biondi, J. P. Bizimana, and D. B. Namanya. Assessing the effects of air temperature and rainfall on malaria incidence: an epidemiological study across Rwanda and Uganda. Geospat. Health, 1:DOI: 10.4081/gh.2016.379, 2016.

F. Di Giuseppe and A. M. Tompkins. Generalizing cloud overlap treatment to include the effect of wind shear. J. Atmos. Sci., 72:2865-2876, 2015.

Christoph Dyroff, Andreas Zahn, Emanuel Christner, Richard Forbes, Adrian M. Tompkins, and Peter F. J. van Velthoven. Comparison of ECMWF analysis and forecast humidity data to CARIBIC upper troposphere and lower stratosphere observations. Q. J. R. Meteorol. Soc., 141:833-844, 2015.

A. M. Tompkins and F. Di Giuseppe. An interpretation of cloud overlap statistics. J. Atmos. Sci., 72:2877-2889, 2015. [http | .pdf]

A. M. Tompkins and F. Di Giuseppe. Potential predictability of malaria using ECMWF monthly and seasonal climate forecasts in Africa. J. Appl. Meteor. Clim, 54:521-540, 2015.

……

Future plans
(Please let us know of any imminent plans regarding a continuation of this research activity, in particular if they are linked to another/new Special Project.)

A project extension has been applied for with the following objectives:

a) Complete the evaluation of the IFS-VECTRI malaria forecasting system in Uganda and carry out similar with colleagues in Senegal as per data availability.

b) Upgrade the VECTRI model version in the system to include improved biting rates and couple the system to the WISDOM population model.

c) Develop products that may be useful for the end-users in Uganda and further countries as deemed appropriate. This is the key focus of the second phase of the project, as our experience in the second phase of the project is that it is extremely difficult to understand and subsequently incorporate climate-related information into the health system decision process effectively. This step will be

approached with a extended visit to Uganda/Senegal by the project PI to work on effective policy integration with local partners.

d) Examine ways of improving the IFS skill over the target regions. In addition to post-processing techniques, we intend to evaluate if key IFS parameter settings (such as CAPE timescales) could be optimally adjusted to improve temperature and rainfall prediction skill over the target area using so-called genetic algorithms. This could turn out to be of more general relevance to improving forecast skill of the IFS.

e) There is currently a version of VECTRI under development to model dengue transmission. If this code is operable within phase 3 of the project, investigations will be made concerning the prediction of dengue over seasonal timescales with partners in the health sector based in India. There is also the possibility to subsequently generalize the code to account for lymphatic filariasis, which is transmitted by similar vectors to malaria.

....

....

This template is available at:
http://www.ecmwf.int/about/computer_access_registration/forms/